SANDIA REPORT
SAND2020-9776
Printed September 2020

Evaluation the Geotech GS-13BH Borehole Seismic Sensor

George W. Slad

Prepared by
Sandia National Laboratories
Albuquerque, New Mexico
87185 and Livermore,
California 94550

Issued by Sandia National Laboratories, operated for the United States Department of Energy by National Technology & Engineering Solutions of Sandia, LLC.

Printed in the United States of America. This report has been reproduced directly from the best available copy.

Available to DOE and DOE contractors from
U.S. Department of Energy
Office of Scientific and Technical Information
P.O. Box 62
Oak Ridge, TN 37831

Telephone: (865) 576-8401
Facsimile: (865) 576-5728
E-Mail: reports@osti.gov
Online ordering: http://www.osti.gov/scitech

Available to the public from
U.S. Department of Commerce
National Technical Information Service
5301 Shawnee Rd
Alexandria, VA 22312

Telephone: (800) 553-6847
Facsimile: (703) 605-6900
E-Mail: orders@ntis.gov
Online order: https://classic.ntis.gov/help/order-methods/

ABSTRACT

Sandia National Laboratories has tested and evaluated the Geotech GS-13BH borehole sensor. The sensor provides a response similar to that of the standard GS-13 short-period seismic sensor intended for pier-installations in a borehole package. The purpose of this seismometer evaluation was to determine a measured sensitivity, amplitude and phase response, self-noise and dynamic range, passband and acceleration response of its calibration coil.

ACKNOWLEDGEMENTS

This work was funded by the United States Department of Energy Office of Nuclear Verification (NA-221).

CONTENTS

LIST OF FIGURES

LIST OF TABLES

ACRONYMS AND DEFINITIONS

dB	Decibel
DOE	Department of Energy
PSD	Power Spectral Density
PSL	Primary Standards Laboratory
SNL	Sandia National Laboratories

INTRODUCTION

The evaluation of Geotech GS-13BH short-period vertical-component sensors serial numbers 101, 102 and 103 were performed to determine the performance characteristics of the sensors. Evaluations of sensitivity, self-noise, dynamic range, frequency response, passband and calibrator response were conducted.

Figure 1 Geotech GS-13BH (Geotech datasheet)

The GS-13BH provides a borehole package design with performance similar to that of a GS-13 seismometer. The sensor has a nominal sensitivity of 2000 V/(m/s), an adjustable natural frequency of 0.75 Hz to 1.05 Hz; see Figure 2 for additional manufacturer-provided specifications.

SHORT-PERIOD SEISMOMETER
MODELS GS-13BH, GS-21 and 20171 SPECIFICATIONS

OPERATING CHARACTERISTICS

Mode of Operation	Vertical, adjustable for tilts up to 10 degrees from vertical
Natural frequency	Adjustable from 0.75 to 1.05 Hz
Inertial mass	5 kg (11.0 lbs.) ±1%
Mass position *vs* temperature	± 1.5 mm over operating temperature range
Dynamic Range	178.4 dB / 164.4 dB / 168.8 dB
Transducer	
Type	Moving coil (velocity)
Damping	Electromagnetic
Generator constant *)	2,000 / 458 / 650 V/(m/s)
Coil Resistance	
GS-13BH	9,100 ohm ±10% (standard) CDR = 81,000 ohm
GS-21	467 ohm ±10% (standard) CDR = 3,400 ohm
20171	6,560 ohm ±10% (standard) CDR = 8,400 ohm
Maximum mass travel	6.4 mm (0.25 in.) pp
Calibration coil	
Motor constant	4.5 / 0.1975 / 0.1975 N/A
Resistance	29 / 24 / 24 ±3 ohm @25°C
Allowable current	
Intantaneous/Sustained	100 mA/10 mA
Temperature range	
Operating	-2 to 49°C (30 to 120°F)

PHYSICAL CHARACTERISTICS

Dimensions (nominal)

Diameter	95 mm (3.75 in.)
Length	98 cm / 118 cm / 118 cm
Net weight	28 kg / 27 kg / 30.8 kg
Shipping weight	45.3 kg (100 lb.)
Shipping volume	0.226 m^3 (8 $ft.^3$)
Seismometer bulk	4.2
Connectors:	
GS-13BH	Receptacle TBD
	Mating plug TBD
GS-21 and 20171	Receptable PT07A-10-6P
	Mating plug PT06W-10-6S

*) Alternate transducer coils are available on special order. Please consult factory for details.

CE

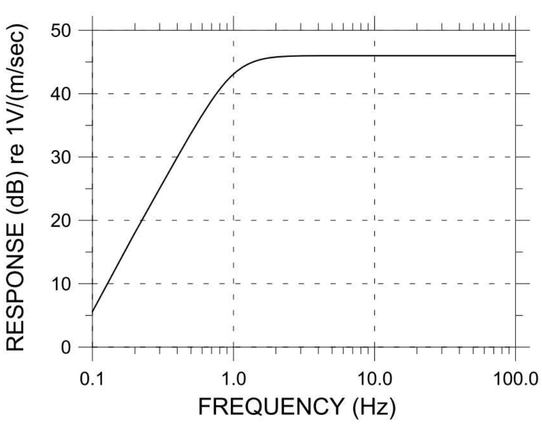

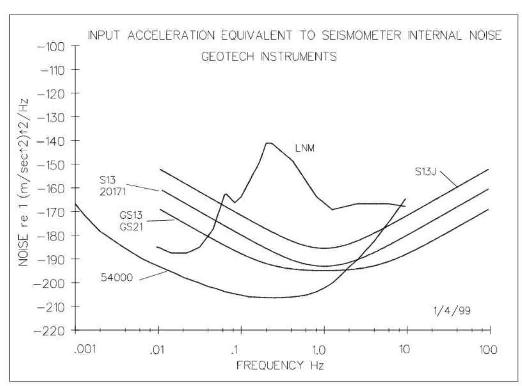

JULY 2009 / DS-GS21&22

SPECIFICATIONS SUBJECT TO CHANGE WITHOUT NOTICE

Figure 2 Seismometer Specifications (Geotech datasheet)

1 TEST PLAN

1.1 Test Facility

Testing of the seismometers was performed at Sandia National Laboratories' Facility for Acceptance, Calibration and Testing (FACT) located near Albuquerque, New Mexico, USA. The FACT site is at approximately 1830 meters in elevation.

Sandia National Laboratories (SNL), Geophysics Department has the capability of evaluating the performance of preamplifiers, digitizing waveform recorders and analog-to-digital converters/high-resolution digitizers for geophysical applications. Tests are based on the Institute of Electrical and Electronics Engineers (IEEE) Standard 1057 for Digitizing Waveform Recorders and Standard 1241 for Analog to Digital Converters. The analyses based on these standards were performed in the frequency domain or time domain as required. When appropriate, instrumentation calibration was traceable to the National Institute for Standards Technology (NIST).

Testing was performed within the FACT site underground bunker due to the bunker's stable temperature, its seismic pier and borehole mounting apparatus.

Figure 3 FACT Site Bunker

The SNL operates a reference seismometer, a Streckheisen STS-2 #120651, which is used to compare against the seismometers under test. All results are made relative to this reference. The reference sensor was recorded at 200 sps by a Quanterra Q330HR, serial number 1551. It is surrounded and covered with cellulose insulation to further improve temperature stability and minimize air convection and is installed within 1 meter of the east wall of the bunker.

1.2 Test Configuration and System Specifications

The Geotech GS-13BH, like its pier variant, the GS-13, is a short-period, passive instrument. The GS-13BH is currently available as a vertical-component-only sensor. The three examples under test were mounted on aluminum extrusions bolted to steel plates anchored to the east bunker wall as shown below.

Figure 4 Geotech GS-13BH sensors

Each sensor was connected to a SMART24B digitizer (Figure 5) for this evaluation, as assigned in the table below.

Table 1 Sensor-Digitizer Assignments

GS-13BH Sensor	SMART-24B digitizer
101	2413
102	2543
103	2454

Figure 5 Representative Geotech SMART-24B Digitizer

The STS-2 reference sensor had been re-calibrated by the USGS Albuquerque Seismic Lab on a Lennartz CT-E1 step calibration table. The resulting sensitivities for the reference STS-2 #120651 are shown below:

Table 2 Reference STS-2 #120651 Sensitivity

Axis	Sensitivity at 1 Hz
Z	1495.51 V/(m/s)

The temperature was maintained to be 23° Celsius with active heating by a radiant electric heater during the spring and early summer. During the summer months, the temperature increased due to ambient conditions and was varied between 23° C and 24° C.

A GPS re-broadcaster operates within the bunker to provide the necessary timing source for the digitizers hosting the reference sensor and sensors under test.

Figure 6 GPS Re-broadcaster

Power to the reference seismic sensor, reference digitizer and host SMART-24B digitizers was provided by the bunker's 300 Amp-Hr photo-voltaic system, supplying a nominal 13.8 VDC during daylight hours.

Before configuring the seismometers for testing, the digitizer bit-weights were calibrated against a reference meter with an active calibration from Sandia's Primary Standards Laboratory. The SNL reference digitizer, Quanterra Q330 #1551 and Geotech SMART-24B dataloggers, #2314, #2453 and #2454 were calibrated using the Agilent 3458A meter #MY45048372. The bit-weights and digitizer channel assignments used are shown in the table below.

Table 3 Testbed Channel Assignments and Digitizer Bit-weights

Model	Serial number	Channel/ Sample Rate (sps)	Bit-weight (40 V_{PP}) gain 16x	Bit-weight (5 V_{PP}) gain 16x	Bit-weight (5 V_{PP}) gain 1x
Q330HR	1551	01HHZ/200	2.3818 uV/count	-	-
SMART-24B	2314	SHZ/200	204.44 nV/count	25.528 nV/count	407.795 uV/count
SMART-24B	2314	SHN/200	-	25.571 nV/count	409.058 uV/count
SMART-24B	2453	SHZ/200	204.93 nV/ count	25.527 nV/count	408.926 uV/count
SMART-24B	2353	SHN/200	-	25.569 nV/count	408.901 uV/count
SMART-24B	2454	SHZ/200	205.53 nV/ count	25.518 nV/count	408.474 uV/count
SMART-24B	2354	SHN/200	-	25.536 nV/count	408.818 uV/count

Each of the SMART-24B digitizers recorded a GS-13BH sensor on their respective SHZ channel. The SMART-24B digitizers were also used to excite the calibration coil of the GS-13BH sensors; when doing so, the SHN channel recorded the signal sent to the calibration coil.

The test configuration was setup consistent with the diagram and descriptions below.

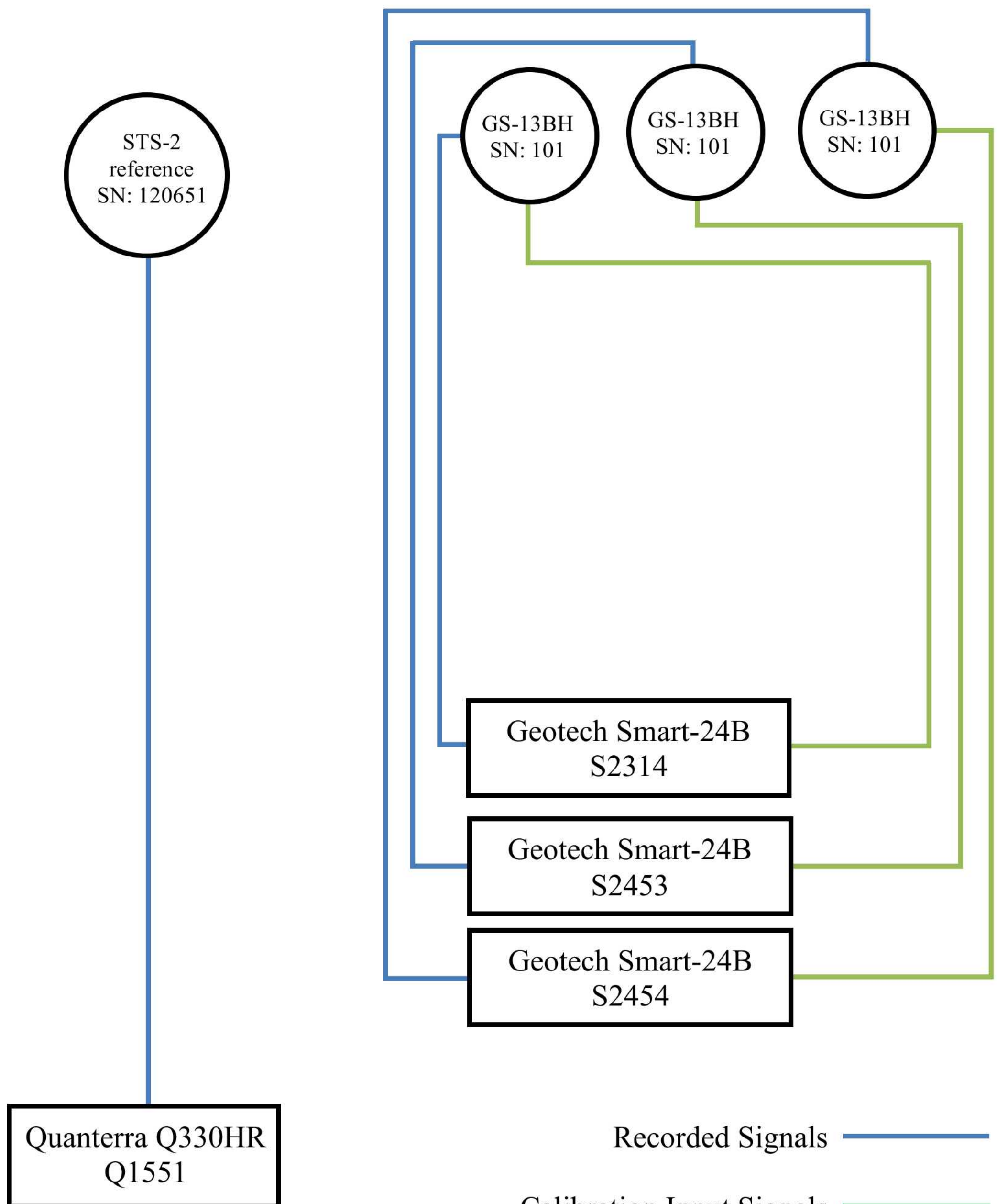

Figure 7 Test Configuration Diagram

1.3 Scope

The following table lists the tests and resulting evaluations that were performed and the configuration of the digitizer.

Table 4 Tests performed

Test	Digitizer Configuration
Sensitivity	40 Vp-p, 16x gain
Self Noise	5 Vp-p, 16x gain
Dynamic Range	5 Vp-p, 16x gain
Frequency Response Verification	40 Vp-p, 16x gain
Passband	40 Vp-p, 16x gain
Calibrator Response Verification	5 Vp-p, 1x gain

1.4 Timeline

Testing of the GS-13BH sensors were performed at Sandia National Laboratories between from May 2020 through August 2020.

1.5 Calibrator Evaluation Frequencies

The calibration coil was excited utilizing the SMART-24B internal calibrator from 0.1 Hz to 25 Hz. Specifically, the frequencies from the function below which generates standardized octave-band values in Hz (ANSI S1.6-1984) with F_0 = 1 Hz:

$$F(n) = F_0 \times 10^{(n/10)}$$

For measurements taken using either broadband or tonal signals, the following frequency values shall be used for n = -20, -19, …, 16, 17. The nominal center frequency values, in Hz, are:

0.10, 0.125, 0.16, 0.20, 0.25, 0.315, 0.40, 0.50, 0.63, 0.8,
1.0, 1.25, 1.6, 2.0, 2.5, 3.15, 4.0, 5.0, 6.3, 8.0,
10.0, 12.5, 16, 20

2 TEST EVALUATION

2.1 Sensitivity

The sensitivity of a sensor is defined to be the "quotient of the change in an indication of a measuring system and the corresponding change in a value of a quantity being measured" (JCGM 200:2012). For a seismometer measuring velocity, the sensitivity value is expressed at a given frequency in units of V/(m/s).

2.1.1 Measurand

The quantity being measured is the sensor's sensitivity at 2.5 Hz in V/(m/s).

2.1.2 Configuration

The sensor under test and a reference sensor with known response characteristics are co-located so that they are both measuring a common earth motion.

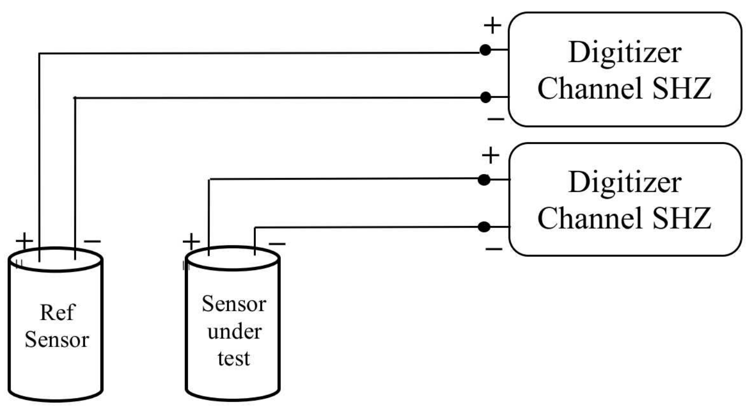

Figure 8 Sensitivity Configuration Diagram

The sensors are allowed to stabilize and then are operated until suitable ground-motion from a local or regional earthquake and/or cultural noise is recorded, to provide high coherence between the sensors.

Table 5 Sensitivity Testbed Equipment

	Manufacturer/Model	Serial Number	Nominal Configuration
Reference Sensor	Streckheisen STS-2	120651	1500 V/(m/s)
Reference Digitizer	Quanterra Q330HR	1551	200 Hz, 40 Vpp
Sensors Under Test	Geotech GS-13BH	101, 102, 103	2000 V/(m/s)
Sensor Digitizer	Geotech SMART-24B	2314, 2453, 2454	200 Hz, 40 Vpp

2.1.3 Analysis and Results

The data recorded using the reference sensor and digitizer has the calibrated bit-weight and sensitivity applied to convert the data to ground motion. The data recorded using the sensor under test and digitizer has just the calibrated bit-weight applied to convert the data to voltage.

The relative transfer function, both amplitude and phase, is computed between the two channels (Merchant, 2011) from the power spectral density:

$$H[k],\ 0 \le k \le N-1$$

The amplitude response at 2.5 Hz is evaluated to compute the sensitivity of the sensor under test.

A combination of a regional earthquake and local cultural noise provided suitable signal to compute the sensitivity at 2.5 Hz. The event utilized is the M_L=6.5, Monte Cristo Range, Nevada, earthquake, which occurred on Friday, May 15, 2020 at 11:03 UTC. The epicenter of this shallow earthquake, 2.7 km depth, is 38.169°N 117.850°W, placing it 1080 km NNW of the FACT site.

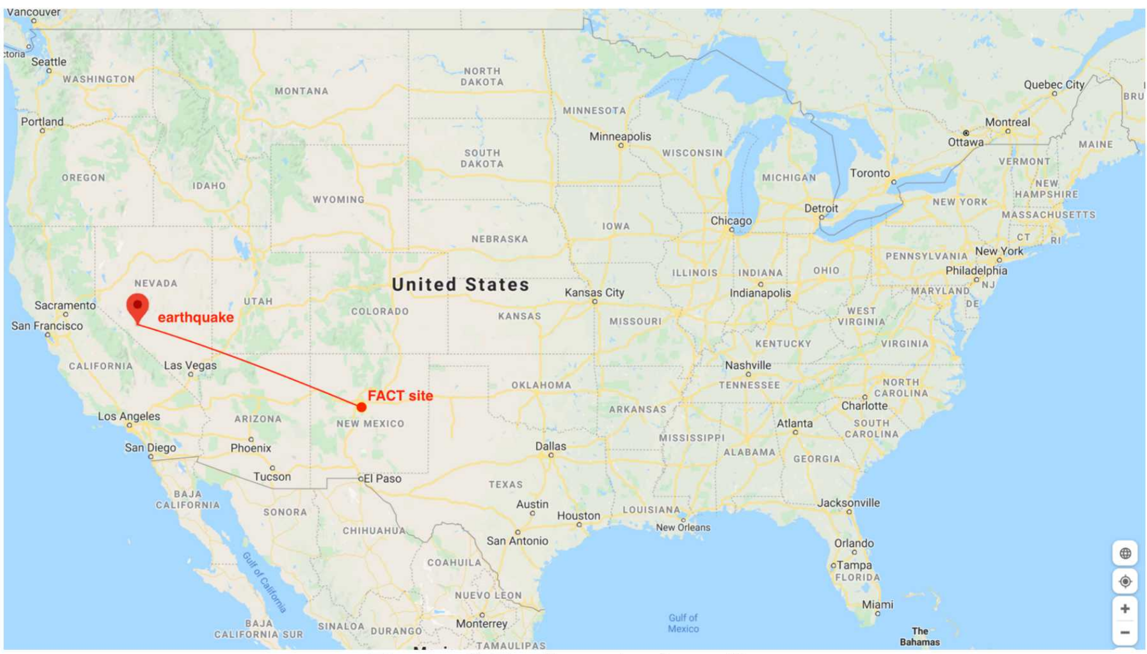

Figure 9 Earthquake Location

The figure below shows the waveform time series utilized for the sensitivity test. Window regions bounded by the red lines indicate the segment of data used for analysis. Notice, following the earthquake, the abundance of signal available to include in the test window. The post-earthquake signal sources are likely vehicles and other cultural noise sources in the vicinity of the FACT site. Recall the broadband response of the STS-2, hence the large amplitude of the lower frequency energy of the P and S waves of the earthquake and the comparatively small amplitude of the cultural noise.

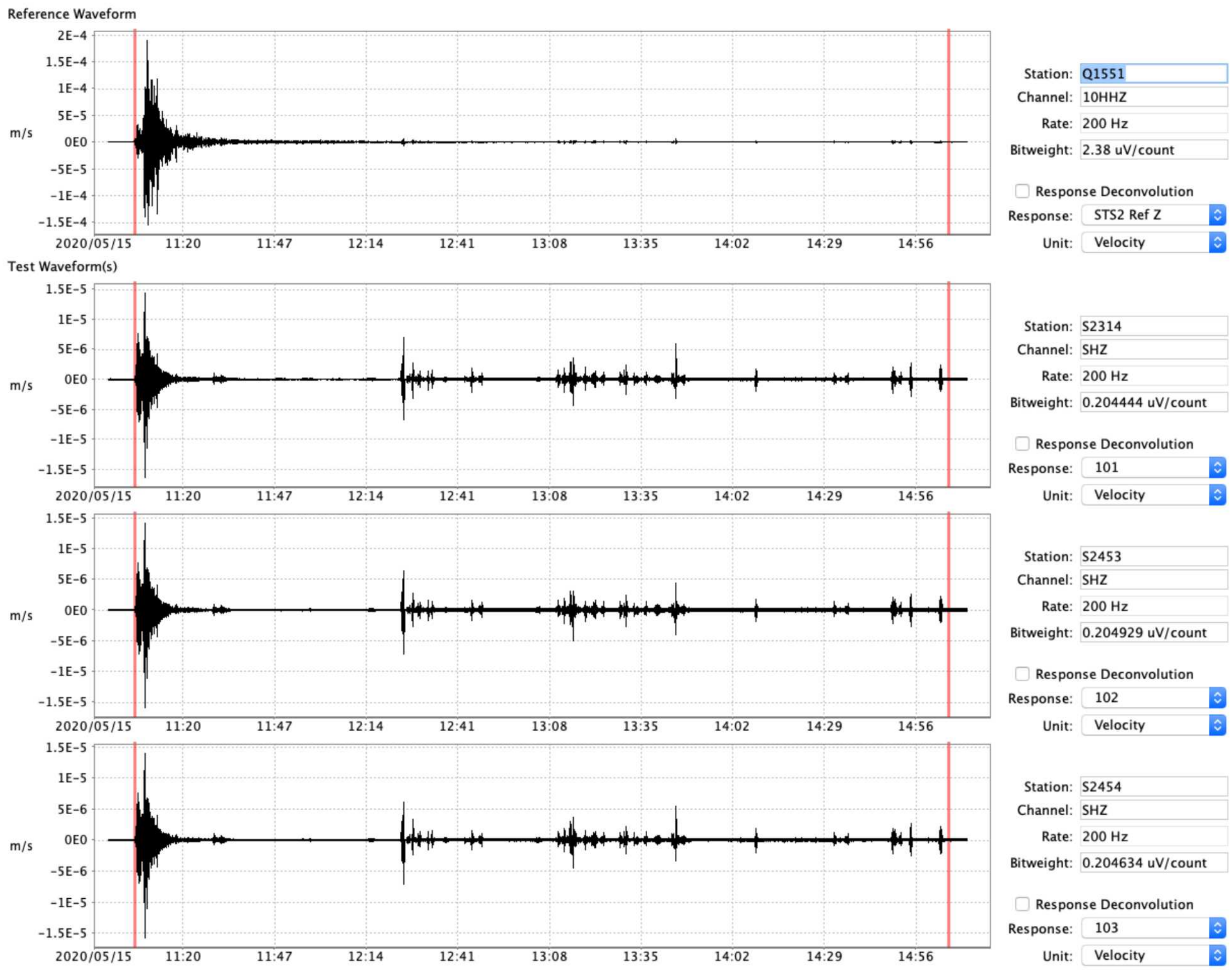

Figure 10 Time Series Utilized for the Sensitivity Test

The figures below show the power spectra, coherence, and amplitude response that were computed from the waveform time series illustrated in Figure 10.

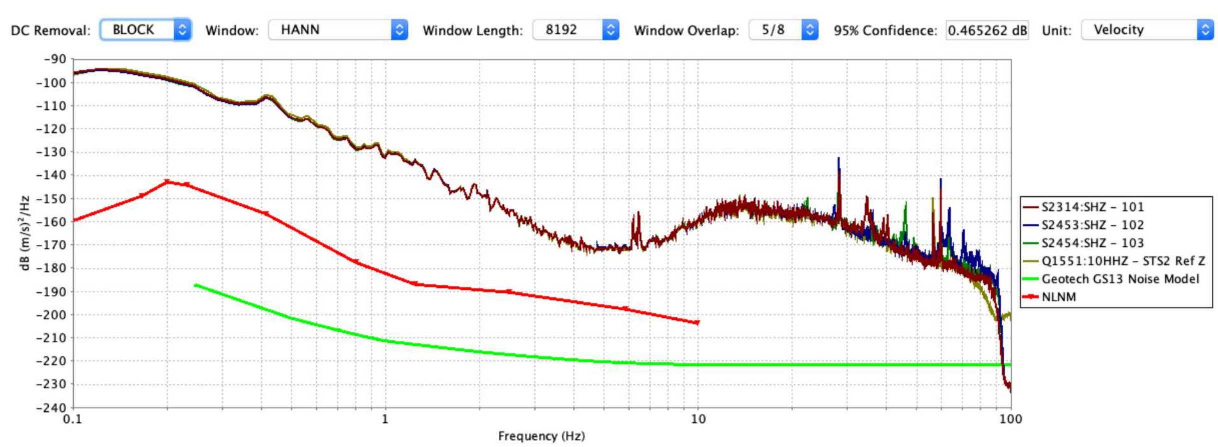

Figure 11 Sensitivity Power Spectra

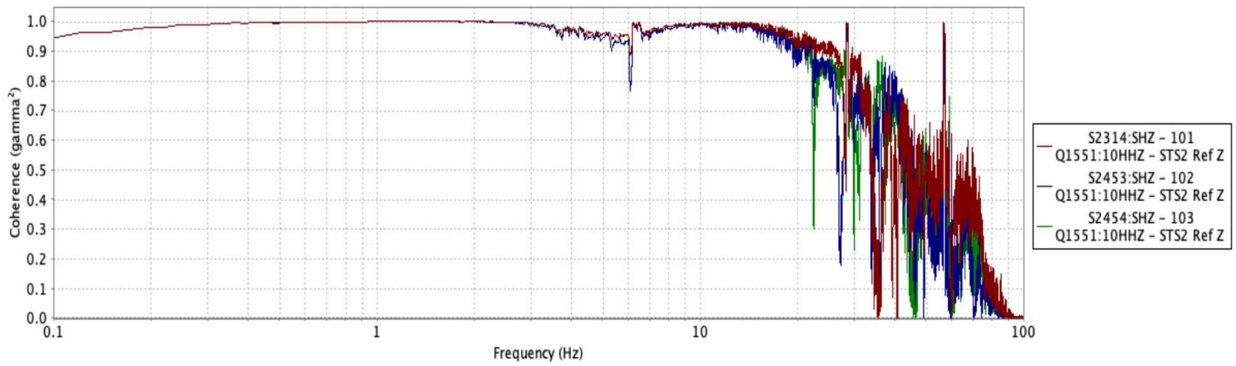

Figure 12 Sensitivity Coherence

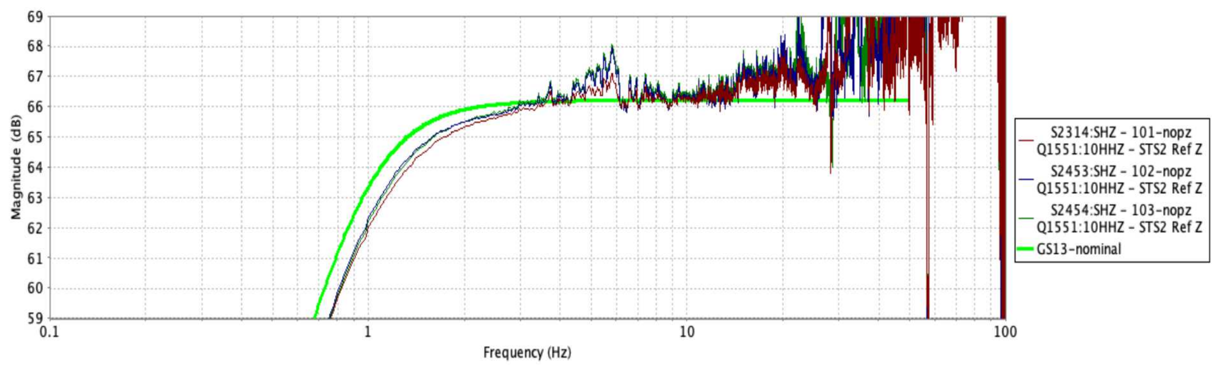

Figure 13 Amplitude Sensitivity Response

Note that the amplitude response curves shown above are consistent with the nominal amplitude response model for a Geotech GS-13, shown in green, with a sensitivity of 2000 V/(m/s) and applied poles and zeros. However, there is a slight shift in each of the amplitude responses at 2.5 Hz, indicating that each seismometer has a unique sensitivity.

The measured sensitivity results, relative to the calibrated reference STS-2 seismometer, are shown in the table below:

Table 6 GS-13BH Sensitivity at 2.5 Hz

Sensor	Nominal	Measured	% Difference
GS-13BH #101	2000 V/(m/s)	1907.8 V/(m/s)	- 4.61%
GS-13BH #102		1932.2 V/(m/s)	- 3.39%
GS-13BH #103		1943.1 V/(m/s)	- 2.84%

Measured sensitivities of the three sensors under test varied from 2.84% to 4.61% below the nominal sensitivity of 2000 V/(m/s) at 2.5 Hz. The Geotech GS-13BH Operation and Maintenance Manual suggests a reduction in sensitivity of approximately 2.3% may be observed if the sensor is placed in direct contact with a steel borehole casing, however, as previously mentioned, the sensors under test were mounted on aluminum extrusions bolted to steel plates which are anchored to the bunker wall (Figure 4). The sensors were not in contact with the steel plates.

Application of the measured sensitivities to the waveform data collected is illustrated below.

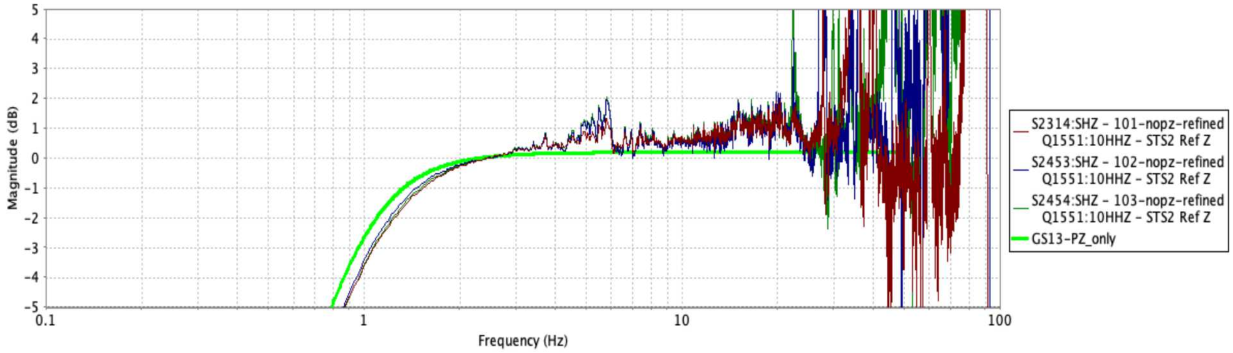

Figure 14 Sensitivity Corrected Amplitude Response

With the measured sensitivities provided in Table 6 applied to the waveform data, the amplitude responses agree well with each other at the calibration frequency of 2.5 Hz.

2.2 Self-Noise

The Self-Noise test measures the amount of noise present on a seismometer by collecting waveform data simultaneously from multiple seismometers during a long-duration, quiet time period. Data are collected from multiple sensors so that coherence analysis may be applied to remove any coherent signal, leaving only incoherence signal, which should approximate the self-noise of the seismometer.

2.2.1 Measurand

The quantity being measured is the sensor's sensitivity at 2.5 Hz in V/(m/s).

2.2.2 Configuration

The sensors under test are co-located so that they are measuring a common earth motion as shown below.

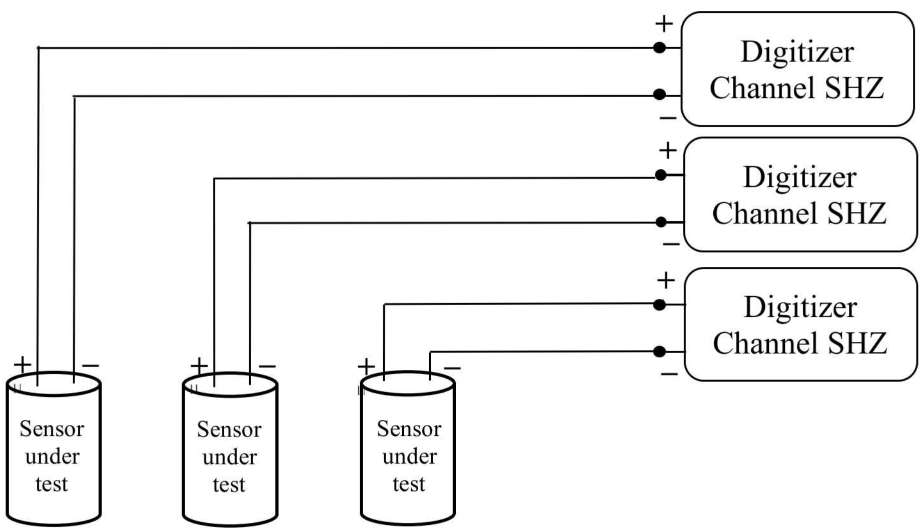

Figure 15 Self-Noise Configuration Diagram

The sensors are allowed to stabilize and then are operated until a suitably quiet, long-duration period is observed, typically overnight or over a weekend. Nearby cultural noise sources, e.g. heating and air conditioning systems are, are temporarily turned off during the time-period.

Table 7 Self Noise Testbed Equipment

	Manufacturer/Model	Serial Number	Nominal Configuration
Sensor under Test	Geotech GS-13BH	101, 102, 103	2000 V/(m/s)
Sensor Digitizer	Geotech SMART-24B	2314, 2453, 2454	5 Vpp with a gain of 16x

The SMART-24B digitizers where reconfigured from 40 Vpp with a gain of 16x to 5 Vpp with a gain of 16x in an attempt to maximize sensor signal over digitizer noise.

2.2.3 Analysis and Results

The data recorded using the sensor under test and digitizer has the calibrated bit-weight, sensitivity, and poles and zeros applied to convert the data to ground motion.

$$x[n], 0 \leq n \leq N\text{–}1$$

The PSD is computed from the time series (Merchant, 2011) from the time series using a 32k-sample Hann window. The window length and data duration were chosen such that there were several points below the lower limit of the evaluation pass-band of 0.5 Hz and the 90% confidence interval of approximately 0.5 dB. The resulting 90% confidence interval was determined to be 0.66 dB.

$$P_{xx}[k], 0 \leq k \leq N - 1$$

Over frequencies (in Hertz):

$$f[k], 0 \leq k \leq N - 1$$

Coherence analysis using the auto and cross power spectra is applied to determine the individual sensor self-noise levels. In the case of two co-located sensors, a 2-channel coherence method (Holcomb, 1989) is used. In the case of three co-located sensors, a 3-channel coherence method (Sleeman, 2007) is used:

$$P_{xx}[k], 0 \leq k \leq N - 1$$

In addition, the total RMS noise over the application pass-band is computed:

$$rms = \sqrt{\frac{1}{T_s L}\sum_{k=n}^{m} |Pxx[k]|}$$

where $f[n]$ and $f[m]$ are the pass $-$ band limits

A review of the data recorded collected determined that a suitable quiet time period occurred August 3, 2020 between approximately 0500 UTC and 1300 UTC, shown below. In local time, this corresponds to an overnight beginning Sunday night, August 3 at 11:00 pm Monday, August 4, 7:00 am.

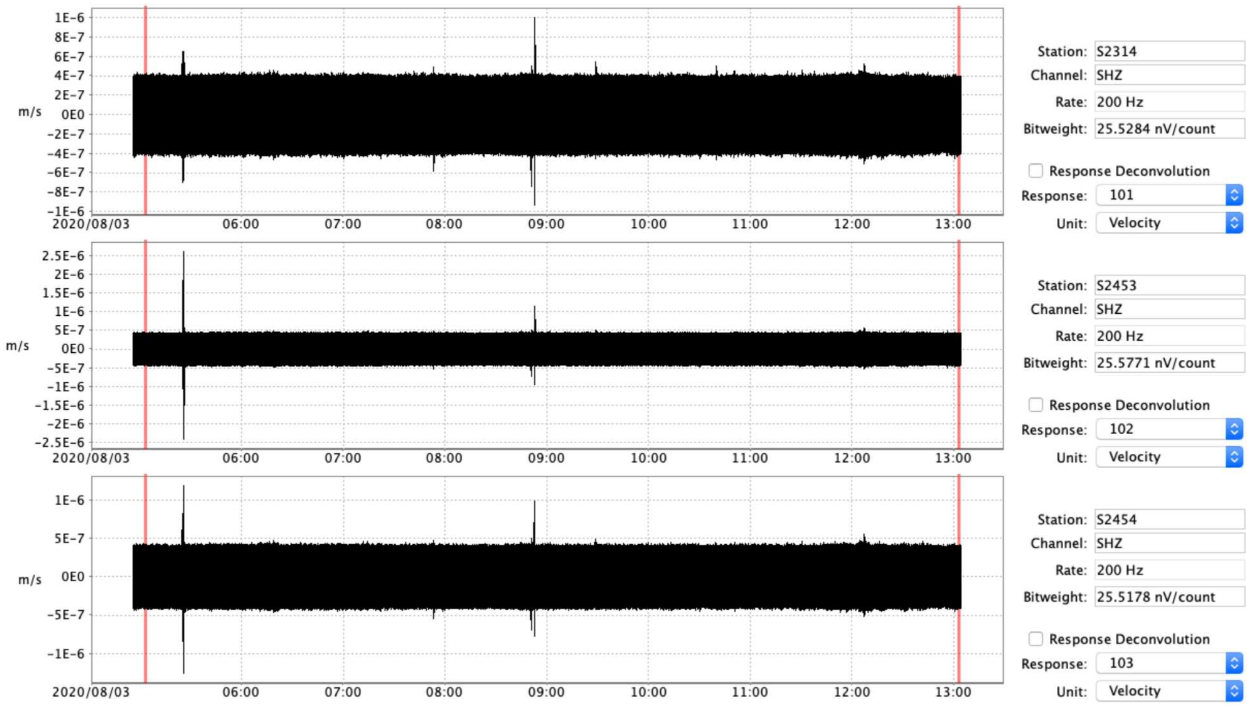

Figure 16 Self-Noise Test Time Series; Digitizer Configuration: 5 Vpp, 16x Gain

The figures below show the raw power spectra, corrected for the individual response models, and the coherence between all combinations of seismometer pairs.

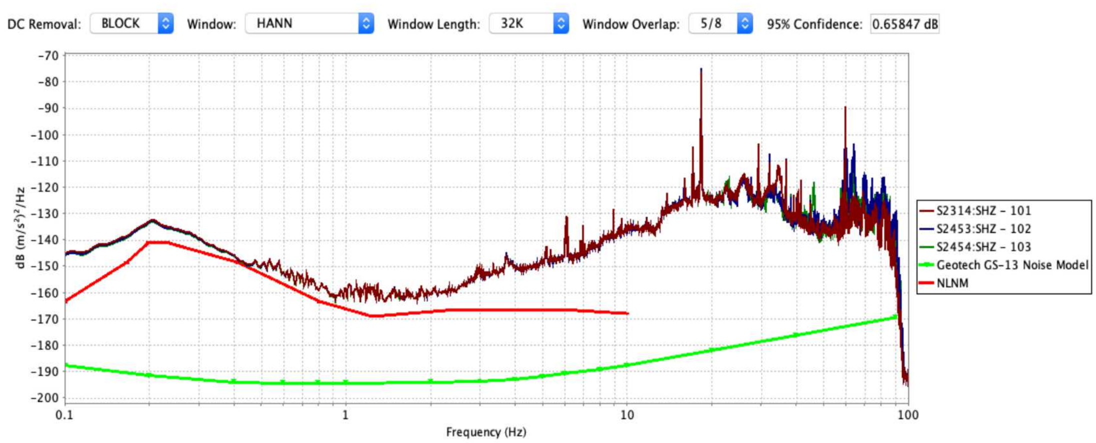

Figure 17 Self-Noise Raw Power Spectra

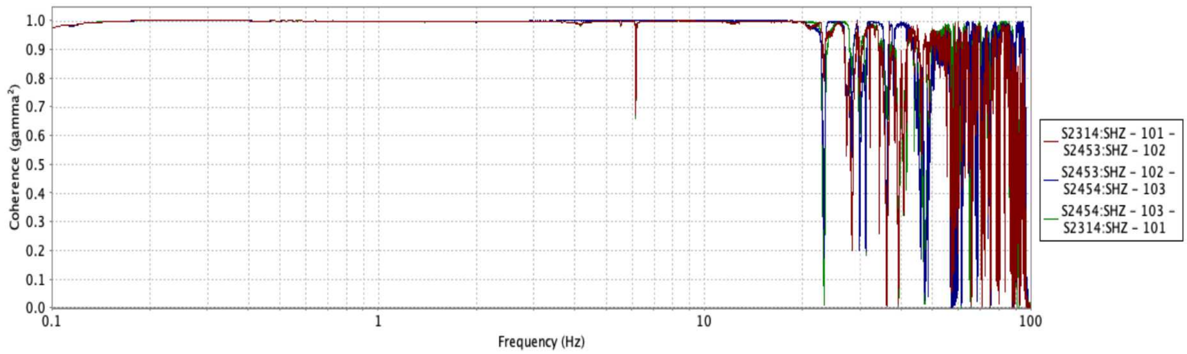

Figure 18 Self-Noise Coherence

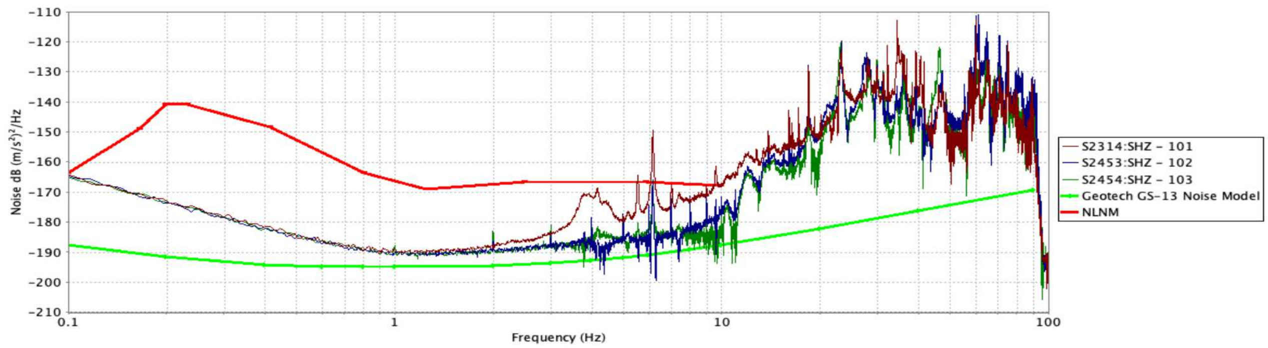

Figure 19 Self-Noise

The self-noise of the sensors follows the GS-13 noise model, at frequencies from 1 to 10 Hz, though it sensor #101 is appreciably higher in this band. Sensor self-noise ranged from 5.1 dB (sensor #102) to 7.1 dB (sensor #103) higher than the noise model at 1 Hz; self-noise at 10 Hz ranged from as little as 5.0 dB higher (sensor #103) to as much as 19.2 dB higher (sensor #101) than that of the noise model. Similar to the coherence observed in the Sensitivity Test, coherence begins to fall off at higher frequencies. Coherence degrades in narrow frequency bands centered at 4.2 Hz, 5.5 Hz, 6.2 Hz, more broadly at 12.8 Hz and at frequencies above 20 Hz.

Table 8 Self-Noise RMS

Sensor	0.5 Hz – 16 Hz
GS-13BH #101	33.3 nm/s^2 rms
GS-13BH #102	19.1 nm/ s^2 rms
GS-13BH #103	14.9 nm/ s^2 rms

The following table contains the seismometer self-noise values from 0.1 Hz to 20 Hz, at 1/3 octave frequency intervals.

Table 9 GS-13BH Self-Noise

Frequency	#101	#102	#103
0.1 Hz	-164.0 dB	-164.2 dB	-164.6 dB
0.125 Hz	-167.7 dB	-166.4 dB	-167.3 dB
0.16 Hz	-170.5 dB	-170.5 dB	-170.5 dB
0.2 Hz	-173.0 dB	-173.8 dB	-173.3 dB
0.25 Hz	-175.4 dB	-176.3 dB	-175.8 dB
0.315 Hz	-178.7 dB	-179.2 dB	-179.3 dB
0.4 Hz	-181.5 dB	-182.0 dB	-182.3 dB
0.5 Hz	-184.9 dB	-184.8 dB	-184.4 dB
0.63 Hz	-187.0 dB	-186.9 dB	-186.8 dB
0.8 Hz	-188.5 dB	-189.3 dB	-189.0 dB
1. Hz	-189.6 dB	-190.3 dB	-190.2 dB
1.25 Hz	-189.7 dB	-190.4 dB	-190.5 dB
1.6 Hz	-189.1 dB	-190.1 dB	-190.3 dB
2. Hz	-187.8 dB	-189.4 dB	-189.7 dB
2.5 Hz	-186.1 dB	-188.6 dB	-188.9 dB
3.15 Hz	-182.9 dB	-187.8 dB	-187.6 dB
4. Hz	-171.5 dB	-187.2 dB	-185.7 dB
5. Hz	-178.0 dB	-185.9 dB	-185.5 dB
6.3 Hz	-174.9 dB	-185.1 dB	-183.6 dB
8. Hz	-172.1 dB	-182.3 dB	-183.8 dB
10. Hz	-166.8 dB	-177.3 dB	-182.8 dB
12.5 Hz	-158.8 dB	-165.0 dB	-166.7 dB
16. Hz	-154.9 dB	-159.6 dB	-162.5 dB
20. Hz	-149.5 dB	-146.3 dB	-151.6 dB

Coherence is likely lost above 20 Hz (Figure 18) due to the seismometers not being perfectly co-located and local site noise resulting in incoherent ground motion observed at the instruments. When applying coherence analysis techniques, it is common for any imperfection in the system (axis alignment, sensor co-location, sensor mounting apparatus, etc.) to result in portions of the recorded signal being incoherent between the sensors.

Sensor self-noise, as best as could be evaluated, is as little as 5.0 dB higher than the GS-13 noise model for sensor #103 and as high as 19.2 dB than the noise model for sensor #101.

2.3 Dynamic Range

Dynamic range is defined to be the ratio between the power of the largest and smallest signals that may be measured.

2.3.1 Measurand

The Dynamic Range is measured as dB of the ratio between the power in the largest and smallest signals. The passive design of the GS-13BH lends itself to providing a voltage output well in excess of a digitizer's input voltage range, therefore the maximum input voltage of the digitizer, as configured for the test (2.5 V_P), will be treated as the largest signal provided by the seismometer, for the purposes of determining dynamic range. The smallest signal is defined to have power equal to the self-noise of the seismometer

2.3.2 Configuration

There is no test configuration for the dynamic range test.

2.3.3 Analysis and Results

The dynamic range over a given pass-band is:

$$Dynamic\ Range = 10 \cdot \log_{10}\left(\frac{signal\ power}{noise\ power}\right)$$

Where

$$signal\ power = \left(fullscale/\sqrt{2}\right)^2$$

$$noise\ power = (RMS\ Noise)^2$$

The application pass-band over which the noise is integrated should be selected to be consistent with the application pass-band.

The RMS noise levels are obtained from the sensor self-noise. The full-scale value utilized, 2.5 V, is the full-scale input of the digitizer as configured for the self-noise test.

Table 10 Dynamic Range

Sensor	0.5 Hz – 16 Hz
GS-13BH #101	112.8 dB
GS-13BH #102	117.6 dB
GS-13BH #103	119.6 dB

Dynamic range values vary most over the frequency range of 0.5 Hz to 16 Hz from 112.8 dB to 119.6 dB; recall sensor 101 had elevated self-noise (Figure 18), relative to the other sensors, from 2 Hz to 18 Hz.

2.4 Frequency Response Verification

The Frequency Response Verification tests measured the amplitude and phase response of a sensor over a frequency band of interest.

2.4.1 Measurand

The quantity being measured is the sensor's amplitude and phase response, relative to the sensitivity at 1 Hz in V/Pa, over a frequency pass-band.

2.4.2 Configuration

The sensor under test and a reference sensor with known response characteristics are co-located so that they are both measuring a common earth motion.

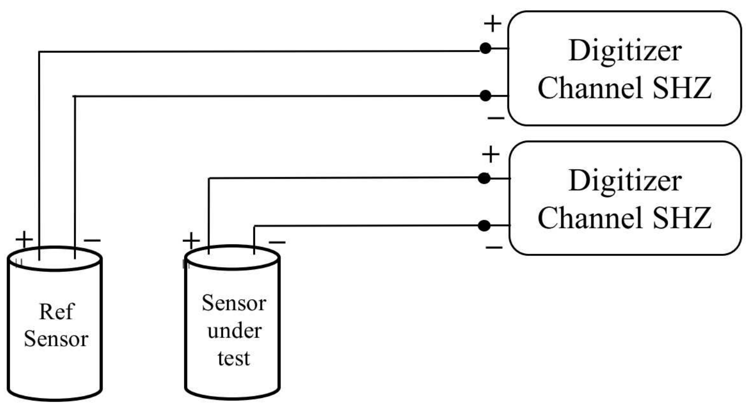

Figure 20 Frequency Response Configuration Diagram

These sensors are allowed to stabilize and then are operated until suitable ground-motion from an earthquake and/or cultural noise is recorded to provide high coherence between the sensors at the calibration frequency of 2.5 Hz.

Table 11 Frequency Response Testbed Equipment

	Manufacturer/Model	Serial Number	Nominal Configuration
Reference Sensor	Streckheisen STS-2	120651	1500 V/(m/s)
Reference Digitizer	Quanterra Q330HR	1551	200 Hz, 40 Vp-p
Sensors Under Test	Geotech GS-13BH	101, 102, 103	2000 V/(m/s)
Sensor Digitizer	Geotech SMART-24B	2314, 2453, 2454	200 Hz, 40 Vp-p

The digitizers record the output of the reference sensor and the sensor under test simultaneously. The reference sensor recording is used for comparison against the sensor-under-test recording.

2.4.3 Analysis and Results

The data recorded using the reference sensor and digitizer has the calibrated bit-weight, sensitivity, and response model applied to convert the data to ground motion.

The data recorded using the sensor under test and digitizer has just the calibrated bit-weight and sensitivity applied to convert the data to ground motion. The response model shape is not applied so that any resulting amplitude or phase response may be observed and compared to the reference.

The relative transfer function, both amplitude and phase, is computed between the two channels (Merchant, 2011) from the power spectral density:

$$H[k],\ 0 \le k \le N-1$$

A four hour window, containing the signal recorded of a large regional earthquake, the Monte Cristo Range, Nevada M_L=6.5 earthquake on May 15, 2020, and numerous nearby cultural noise sources recorded early during the work day, provides the energy source to verify the GS-13BH sensors' response. Refer to section 2.1.3 for a map of the earthquake in relation to the FACT site and a time-series plot of the data.

The following figures and tables contain the seismometer response values as calculated when compared to the STS-2 reference seismometer.

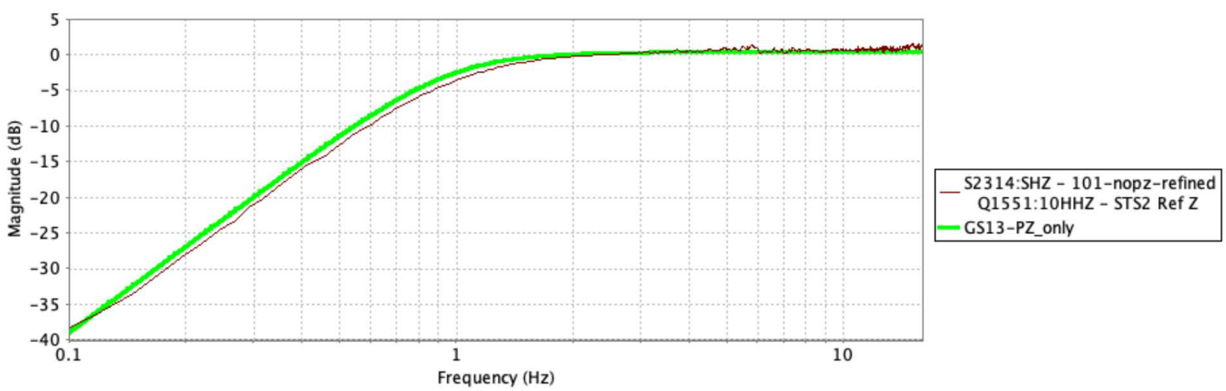

Figure 21 Sensor 101 Amplitude Response

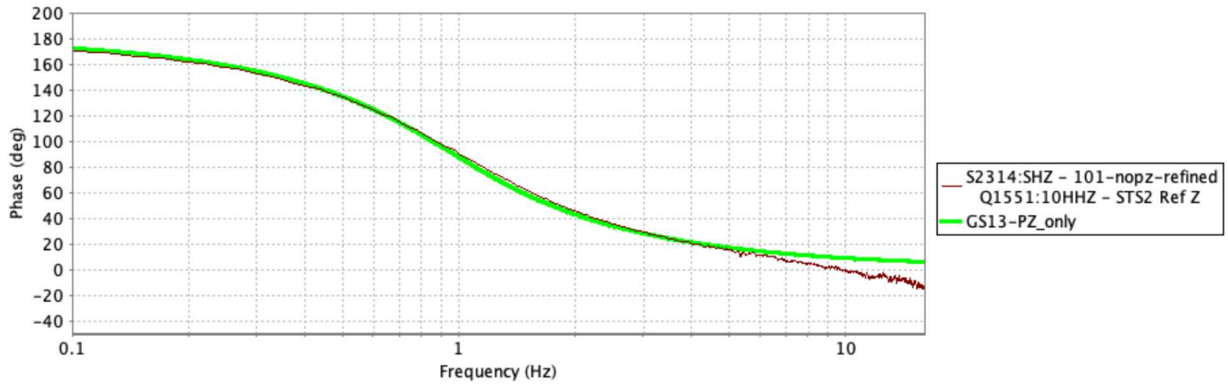

Figure 22 Sensor 101 Phase Response

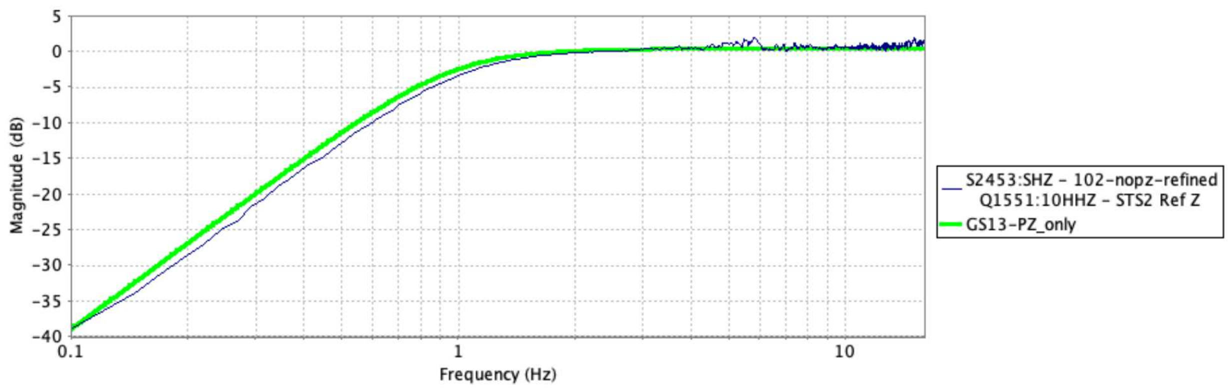

Figure 23 Sensor 102 Amplitude Response

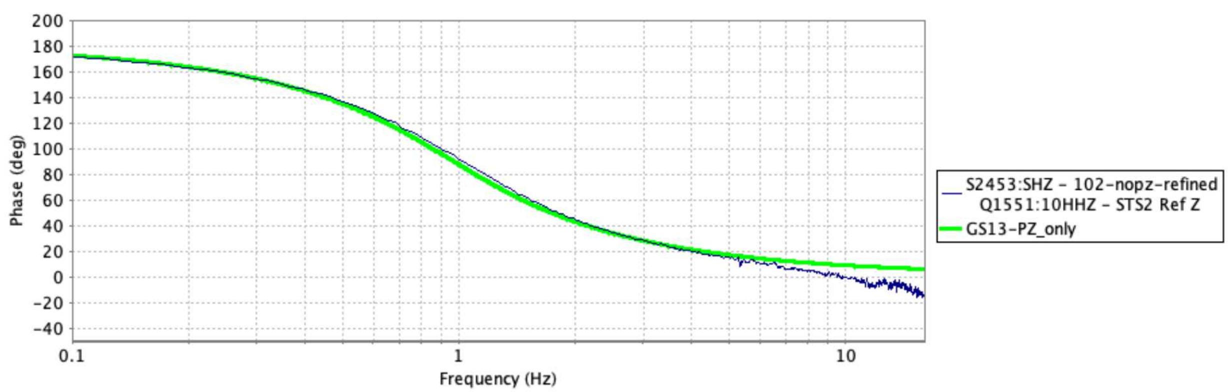

Figure 24 Sensor 102 Phase Response

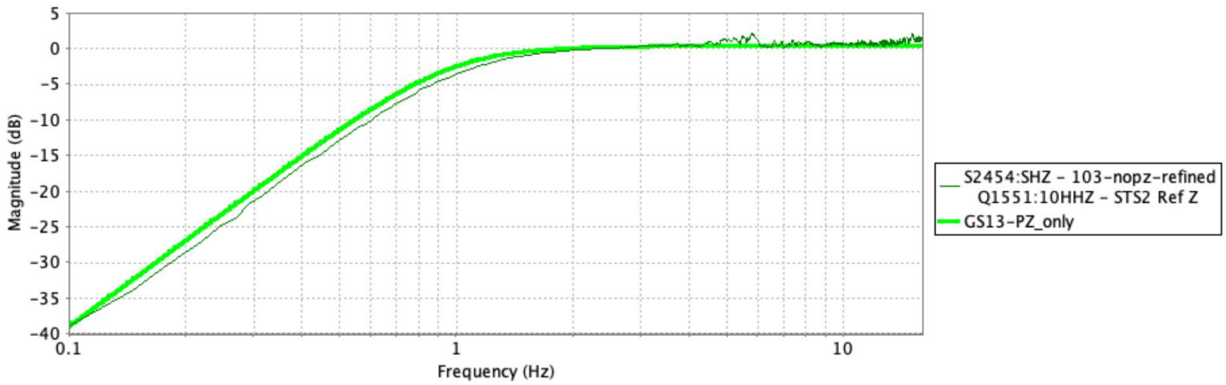

Figure 25 Sensor 103 Amplitude Response

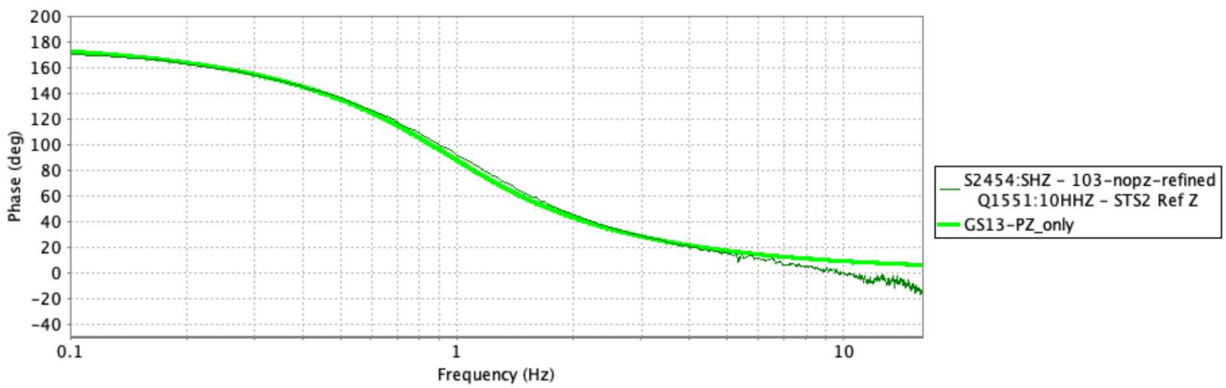

Figure 26 Sensor 101 Phase Response

The regional earthquake and cultural noise signals utilized in the test provided a high amplitude, highly coherent signal, especially at the lower frequencies of interest, allowing for high confidence measurements of the sensor response. Recall though, from section 2.1.3, coherence degrades at higher frequencies. Coherence drops below ideal levels between approximately 3.5 Hz and 7 Hz (Figure 12); the variation in amplitude and phase in these regions in these amplitude and phase responses plots should be viewed with this in mind.

Table 12 Amplitude and Phase Response, All Sensors

Frequency	Sensor 101		Sensor 102		Sensor 103	
	Amplitude	Phase	Amplitude	Phase	Amplitude	Phase
0.1 Hz	-38.66 dB	169.76 deg	-39.17 dB	170.56 deg	-39.15 dB	169.98 deg
0.125 Hz	-35.89 dB	169.76 deg	-36.40 dB	170.56 deg	-36.39 dB	169.98 deg
0.16 Hz	-30.82 dB	164.85 deg	-31.31 dB	166.07 deg	-31.29 dB	165.42 deg
0.2 Hz	-28.42 dB	161.65 deg	-28.89 dB	163.05 deg	-28.88 dB	162.43 deg
0.25 Hz	-24.62 dB	157.87 deg	-25.06 dB	159.52 deg	-25.07 dB	158.84 deg
0.315 Hz	-20.29 dB	151.10 deg	-20.68 dB	153.15 deg	-20.71 dB	152.44 deg
0.4 Hz	-16.46 dB	143.92 deg	-16.78 dB	146.40 deg	-16.83 dB	145.78 deg
0.5 Hz	-13.04 dB	134.90 deg	-13.26 dB	137.65 deg	-13.35 dB	137.04 deg
0.63 Hz	-8.99 dB	120.97 deg	-9.06 dB	123.76 deg	-9.19 dB	123.31 deg
0.8 Hz	-5.90 dB	105.93 deg	-5.81 dB	108.29 deg	-5.97 dB	108.09 deg
1 Hz	-3.58 dB	89.75 deg	-3.37 dB	91.19 deg	-3.54 dB	91.41 deg
1.25 Hz	-2.02 dB	74.53 deg	-1.80 dB	74.89 deg	-1.94 dB	75.40 deg
1.6 Hz	-0.83 dB	57.94 deg	-0.68 dB	57.35 deg	-0.75 dB	58.11 deg
2 Hz	-0.29 dB	45.51 deg	-0.24 dB	44.51 deg	-0.28 dB	45.28 deg
2.5 Hz	0.00 dB	35.84 deg	0.00 dB	34.75 deg	0.00 dB	35.37 deg
3.15 Hz	0.27 dB	27.49 deg	0.29 dB	26.65 deg	0.32 dB	27.40 deg
4 Hz	0.43 dB	20.32 deg	0.37 dB	19.89 deg	0.41 dB	20.15 deg
5 Hz	0.73 dB	15.23 deg	1.00 dB	15.05 deg	1.06 dB	15.14 deg
6.3 Hz	0.50 dB	10.43 deg	0.48 dB	10.18 deg	0.54 dB	10.37 deg
8 Hz	0.56 dB	4.66 deg	0.49 dB	4.73 deg	0.57 dB	4.90 deg
10 Hz	0.59 dB	-0.78 deg	0.53 dB	-0.51 deg	0.59 dB	-0.65 deg
12.5 Hz	0.72 dB	-5.75 deg	0.59 dB	-5.51 deg	0.71 dB	-5.37 deg
16 Hz	1.15 dB	-13.72 deg	1.17 dB	-14.09 deg	1.27 dB	-14.12 deg
20 Hz	1.06 dB	-22.08 deg	1.04 dB	-23.54 deg	1.14 dB	-23.84 deg

The measured amplitude and phase responses of GS-13BH sensors agree with GS-13 response model over frequencies associated with high coherence. Sensor amplitude response varied no more than -0.33 dB (sensor 101) from the average, at 0.1 Hz, well outside of the GS-13BH passband.

2.5 Passband

The Passband test measures the bandwidth of the seismometer determined from the measured amplitude response.

2.5.1 Measurand

The quantity being measured is the low and high frequency limits of the sensor's passband.

2.5.2 Configuration

The sensor under test and a reference sensor with known response characteristics are co-located so that they are both measuring a common earth motion.

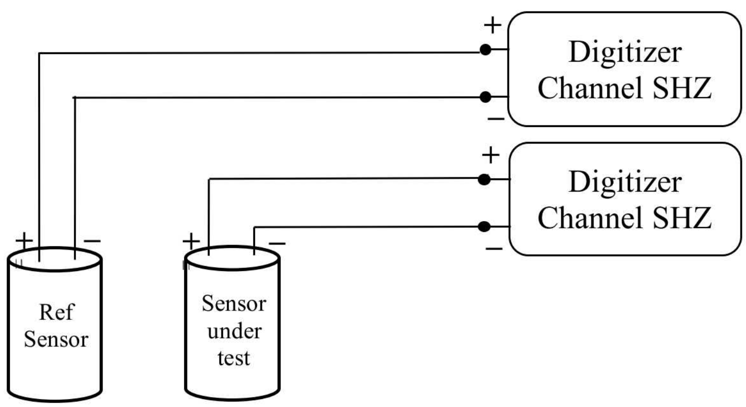

Figure 27 Passband Configuration Diagram

The sensors are allowed to stabilize and then are operated until suitable ground-motion from an earthquake and/or cultural noise is recorded to provide high coherence.

Table 13 Passband Testbed Equipment

	Manufacturer/Model	Serial Number	Nominal Configuration
Reference Sensor	Streckheisen STS-2	120651	1500 V/(m/s)
Reference Digitizer	Quanterra Q330HR	1551	200 Hz, 40 Vpp
Sensors Under Test	Geotech GS-13BH	101, 102, 103	2000 V/(m/s)
Sensor Digitizer	Geotech SMART-24B	2314, 2453, 2454	200 Hz, 40 Vpp

The digitizers record the output of the reference sensor and the sensor under test simultaneously. The reference sensor recording is used for comparison against the sensor-under-test recording.

2.5.3 Analysis and Results

The data recorded using the reference sensor and digitizer has the calibrated bit-weight, sensitivity, and response model applied to convert the data to ground motion.

The data recorded using the sensor under test and digitizer has just the calibrated bit-weight and sensitivity applied to convert the data to ground motion. The response model shape is not applied so that any resulting amplitude or phase response may be observed and compared to the reference.

The relative transfer function, both amplitude and phase, is computed between the two channels (Merchant, 2011) from the power spectral density:

$$H[k],\ 0 \le k \le N-1$$

The frequencies at which the response is down 3 dB are measured.

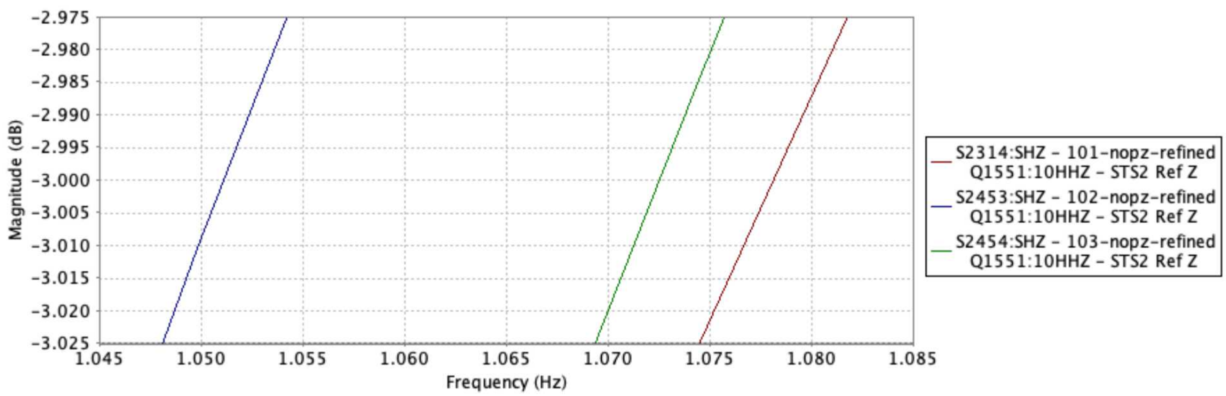

Figure 28 Passband Low Passband Limit

Table 14 Passband Limits

	Sensor 101	Sensor 102	Sensor 103
Low Frequency	1.08 Hz	1.05 Hz	1.07 Hz
High Frequency	> 20 Hz	> 20 Hz	> 20 Hz

High coherence at lower frequencies allows for a precise measurement of the low frequency limit of the passband. As previously discussed, limits of coherence between the reference and sensors under test at higher frequencies limits any determination of passband above 20 Hz. As expected, at 20 Hz there is no evidence of amplitude response roll-off indicating any upper limit in passband near 20 Hz.

The low frequency passband limit of the sensors under test varied from 1.05 Hz to 1.08 Hz.

2.6 Calibrator Response

The Calibrator Response test is used to measure the sensitivity of the seismometer calibrator over a range of frequencies.

2.6.1 Measurand

The quantity being measured is the seismometer calibration coil sensitivity over select frequencies, from 0.1 Hz to 25 Hz, at 1/3 octave intervals, as described Section 1.5.

2.6.2 Configuration

The seismometer is connected to a digitizer.

A signal generator, or in this case, the digitizer's calibrator circuit, generates a voltage of known frequency and amplitude which is applied to the calibration coil of the sensor-under-test to excite the mass of the sensor.

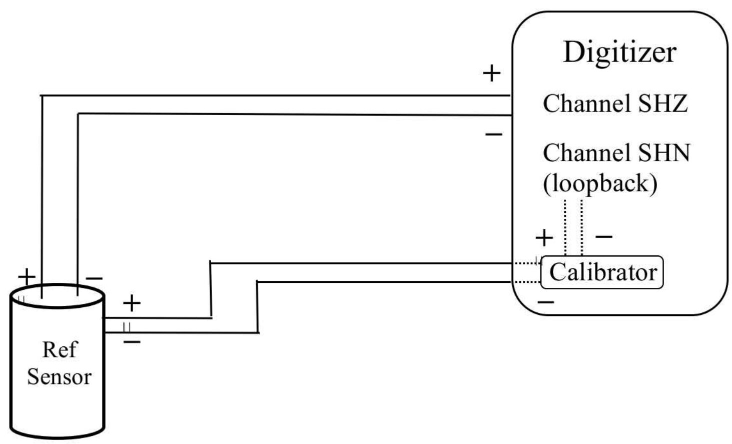

Figure 29 Calibrator Response Configuration Diagram

The digitizer records both the output of the sensor under test and the output of the calibrator circuit, which serves as the input to the calibration coil of the sensor under test, simultaneously, as shown in Figure 29.

The digitizer is configured as shown in Table 15 below.

Table 15 Calibrator Response Testbed Equipment

	Manufacturer/Model	Serial Number	Nominal Configuration
Sensors Under Test	Geotech GS-13BH	101, 102, 103	2000 V/(m/s)
Sensor Digitizer	Geotech SMART-24B	2314, 2453, 2454	200 Hz, 5 Vp-p

2.6.3 Analysis and Results

The digitizer calibrator excites the cal coil, at discrete frequencies from 0.1 Hz to 25 Hz. A minimum of 5 cycles of data is defined in both the sensor velocity output time-series, channel SHZ, and the calibrator loopback recording, channel SHN.

A four parameter sine fit (Merchant, 2011; IEEE-STD1281) is applied to the time segments from the digitizer channels in Counts in order to determine the sinusoid's amplitude, frequency, phase, and DC offset:

$$V_{in}\sin\left(2\pi f_{in}t + \theta_{calibrator}\right) + V_{dc\ in}$$

$$V_{out}\sin(2\pi f_{out}t + \vartheta_{meas}) + V_{dc\ out}$$

The seismometer calibrator sensitivity in (m/s^2)/V is computed:

$$G_{calib} = \frac{\frac{V_{out}}{G_{seis}} * 2\pi f}{V_{in}}$$

The SMART-24B digitizer provides a means to generate sine calibration signals with user-configurable amplitude, frequency and duration. Initial tests were conducted with a digitizer gain of 16x while the calibrator provided a signal amplitude of 0.25 V peak. During analysis after the initial tests, it was found insufficient signal to noise existed after the velocity output was differentiated into acceleration, in particular at higher frequencies. To improve the signal to noise, the gain of the digitizer was reduced from 16x to 1x to allow the sensor's mass to be driven with a higher voltage calibration signal so it may in turn provide a larger output amplitude, thereby improving the signal to noise of the measured output after differentiation from velocity to acceleration.

Example time-series of the calibrator input loopback (to channel SHN) and the resulting output on channel SHZ, converted to acceleration, are shown below.

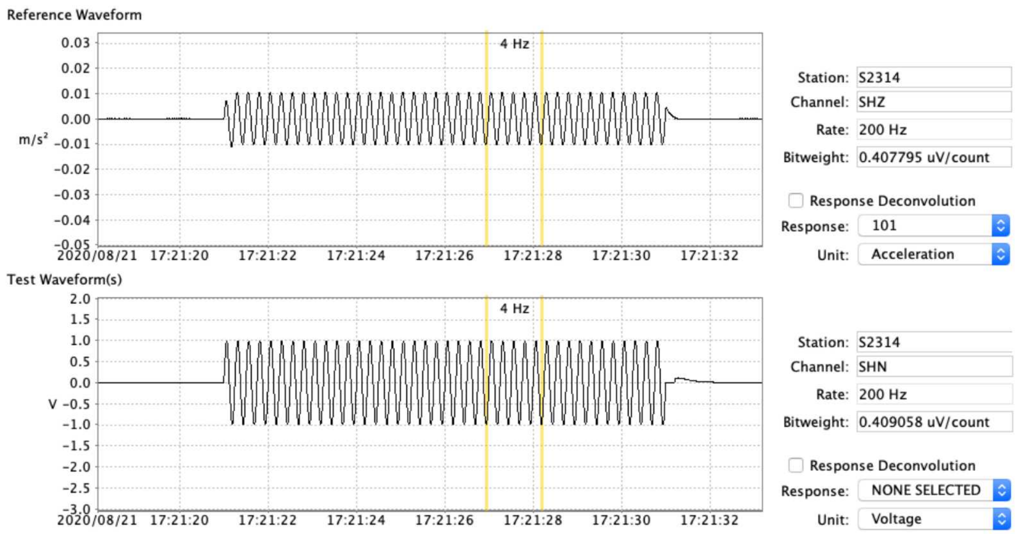

Figure 30 Example Calibrator Response Timeseries

By exciting the calibration coil of each sensor, over the aforementioned range of frequencies, calibration coil acceleration response curves may be generated, as shown below.

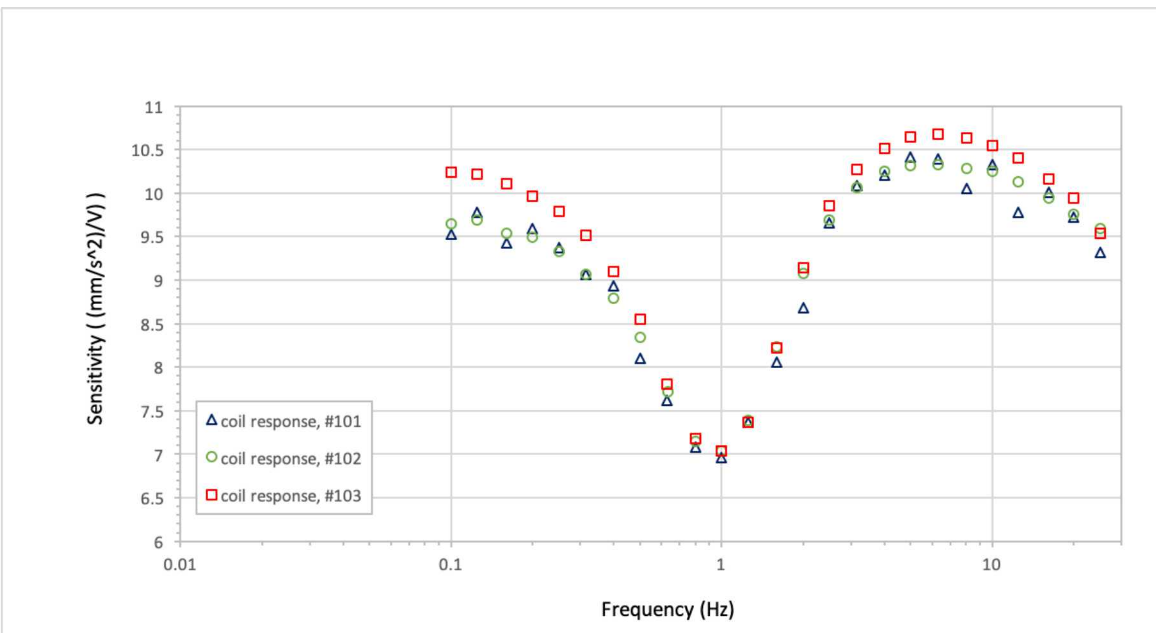

Figure 31 Sensor Calibration Coil Acceleration Response

Calibration coil responses vary between sensors, generally most at the lowest frequencies, though at 8 Hz and 12.5 Hz calibration coil responses vary between sensors 101 and 103 as much as the coil response does at 0.1 Hz and 0.16 Hz. Signal to noise ratios of the data collected for sensor 101 (digitizer 2314) proved to be notably lower than that of the other two sensors' waveforms. The variation in acceleration response calculated, in particular at 8 Hz and 12.5 Hz may be affected by the lower signal to noise ratio of the data.

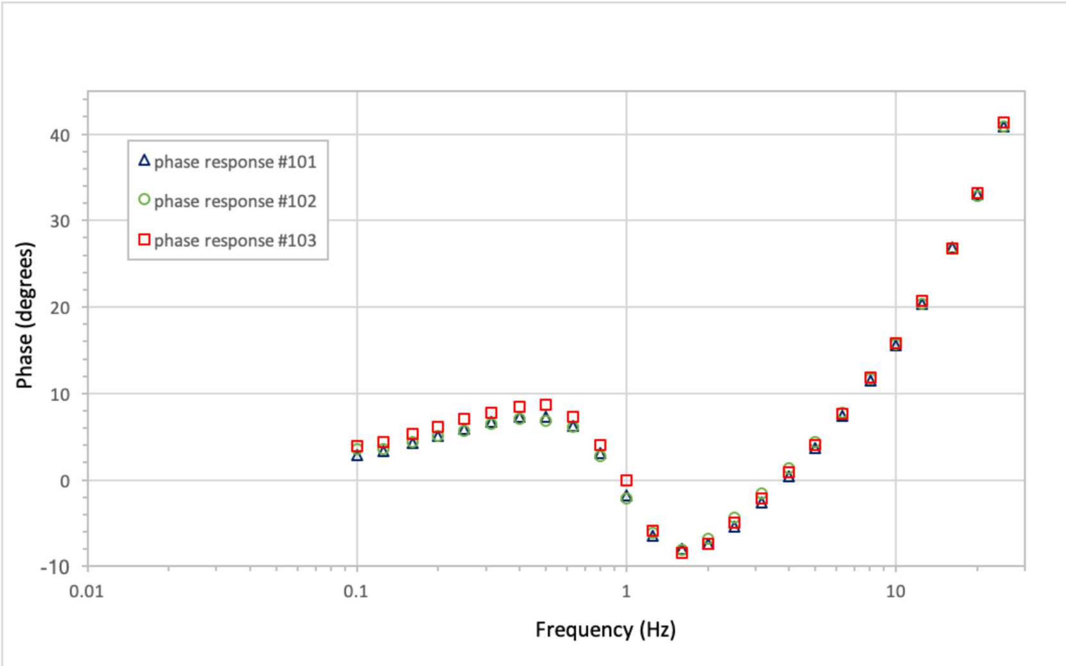

Figure 32 Sensor Calibration Coil Phase Response

Calibration coil phase response across the sensors are very similar; though the phase response of sensor 101's calibration coil deviates slightly from the other two calibration coil phase responses between 0.16 Hz and 1.0 Hz as the phase response of sensors 102 and 103 essentially overlay each other over this range of frequencies.

Table 16 Calibration Coil Acceleration Response

Nominal Frequency	Sensor 101	Sensor 102	Sensor 103
0.1 Hz	9.521 (mm/s^2)/V	9.649 (mm/s^2)/V	10.238 (mm/s^2)/V
0.125 Hz	9.779 (mm/s^2)/V	9.696 (mm/s^2)/V	10.216 (mm/s^2)/V
0.16 Hz	9.424 (mm/s^2)/V	9.538 (mm/s^2)/V	10.102 (mm/s^2)/V
0.2 Hz	9.591 (mm/s^2)/V	9.490 (mm/s^2)/V	9.969 (mm/s^2)/V
0.25 Hz	9.378 (mm/s^2)/V	9.329 (mm/s^2)/V	9.790 (mm/s^2)/V
0.315 Hz	9.060 (mm/s^2)/V	9.063 (mm/s^2)/V	9.512 (mm/s^2)/V
0.4 Hz	8.932 (mm/s^2)/V	8.792 (mm/s^2)/V	9.104 (mm/s^2)/V
0.5 Hz	8.104 (mm/s^2)/V	8.340 (mm/s^2)/V	8.550 (mm/s^2)/V
0.63 Hz	7.624 (mm/s^2)/V	7.717 (mm/s^2)/V	7.808 (mm/s^2)/V
0.8 Hz	7.086 (mm/s^2)/V	7.150 (mm/s^2)/V	7.185 (mm/s^2)/V
1.0 Hz	6.962 (mm/s^2)/V	7.044 (mm/s^2)/V	7.038 (mm/s^2)/V
1.25 Hz	7.367 (mm/s^2)/V	7.384 (mm/s^2)/V	7.366 (mm/s^2)/V
1.6 Hz	8.063 (mm/s^2)/V	8.233 (mm/s^2)/V	8.221 (mm/s^2)/V
2.0 Hz	8.678 (mm/s^2)/V	9.075 (mm/s^2)/V	9.140 (mm/s^2)/V
2.5 Hz	9.662 (mm/s^2)/V	9.687 (mm/s^2)/V	9.857 (mm/s^2)/V
3.15 Hz	10.088 (mm/s^2)/V	10.059 (mm/s^2)/V	10.272 (mm/s^2)/V
4.0 Hz	10.207 (mm/s^2)/V	10.247 (mm/s^2)/V	10.514 (mm/s^2)/V
5.0 Hz	10.409 (mm/s^2)/V	10.316 (mm/s^2)/V	10.639 (mm/s^2)/V
6.3 Hz	10.392 (mm/s^2)/V	10.321 (mm/s^2)/V	10.675 (mm/s^2)/V
8 Hz	10.048 (mm/s^2)/V	10.287 (mm/s^2)/V	10.637 (mm/s^2)/V
10 Hz	10.324 (mm/s^2)/V	10.246 (mm/s^2)/V	10.548 (mm/s^2)/V
12.5 Hz	9.773 (mm/s^2)/V	10.128 (mm/s^2)/V	10.408 (mm/s^2)/V
16 Hz	10.006 (mm/s^2)/V	9.940 (mm/s^2)/V	10.167 (mm/s^2)/V
20 Hz	9.722 (mm/s^2)/V	9.758 (mm/s^2)/V	9.940 (mm/s^2)/V
25 Hz	9.321 (mm/s^2)/V	9.595 (mm/s^2)/V	9.537 (mm/s^2)/V

Calibration coil acceleraton response varied from 4.44% lower to as much as 3.2% higher than the average over the three sensors at any given frequency. The largest variation of 4.44%, observed in sensor 103, occurred well outside of the seismometer's passband, at 0.1 Hz.

Table 17 Calibration Coil Phase Response

Nominal Frequency	Sensor 101	Sensor 102	Sensor 103
0.1 Hz	2.81 deg	3.54 deg	3.88 deg
0.125 Hz	3.37 deg	3.55 deg	4.34 deg
0.16 Hz	4.22 deg	4.41 deg	5.35 deg
0.2 Hz	5.09 deg	5.07 deg	6.15 deg
0.25 Hz	5.93 deg	5.66 deg	7.12 deg
0.315 Hz	6.77 deg	6.49 deg	7.77 deg
0.4 Hz	7.33 deg	7.03 deg	8.46 deg
0.5 Hz	7.25 deg	6.80 deg	8.66 deg
0.63 Hz	6.22 deg	6.18 deg	7.27 deg
0.8 Hz	3.08 deg	2.71 deg	4.01 deg
1.0 Hz	-1.79 deg	-2.16 deg	-0.10 deg
1.25 Hz	-6.49 deg	-6.07 deg	-5.90 deg
1.6 Hz	-7.98 deg	-8.06 deg	-8.39 deg
2.0 Hz	-7.39 deg	-6.85 deg	-7.40 deg
2.5 Hz	-5.39 deg	-4.39 deg	-4.91 deg
3.15 Hz	-2.63 deg	-1.62 deg	-2.13 deg
4.0 Hz	0.46 deg	1.30 deg	0.89 deg
5.0 Hz	3.69 deg	4.35 deg	4.06 deg
6.3 Hz	7.40 deg	7.82 deg	7.68 deg
8 Hz	11.50 deg	11.73 deg	11.82 deg
10 Hz	15.63 deg	15.74 deg	15.82 deg
12.5 Hz	20.39 deg	20.33 deg	20.73 deg
16 Hz	26.94 deg	26.81 deg	26.83 deg
20 Hz	33.02 deg	32.79 deg	33.22 deg
25 Hz	40.86 deg	40.92 deg	41.33 deg

3 SUMMARY

Sensitivity
Measured sensitivities of the three sensors under test varied from 2.84% to 4.61% below the nominal sensitivity of 2000 V/(m/s) at 2.5 Hz.

Self-Noise
Sensor self-noise, as best as could be evaluated, is as little as 5.0 dB higher than the GS-13 noise model for sensor #103 and as high as 19.2 dB than the noise model for sensor #101.

Dynamic Range
Dynamic range values vary most over the frequency range of 0.5 Hz to 16 Hz from 112.8 dB to 119.6 dB.

Frequency Response Verification
The measured amplitude and phase responses of GS-13BH sensors agree with GS-13 response model over frequencies associated with high coherence. Sensor amplitude response varied no more than -0.33 dB (sensor 101) from the average, at 0.1 Hz, well outside of the GS-13BH passband.

Passband
The low frequency passband limit of the sensors under test varied from 1.05 Hz to 1.08 Hz.

Calibrator Response
Calibration coil acceleraton response varied from 4.44% lower to as much as 3.2% higher than the average over the three sensors at any given frequency. Calibration coil phase response varied most from the average for any given frequency at 1.0 Hz, where sensor 103's phase is -0.10 degrees; the average across all sensors at 1 Hz was -1.35 degrees.

REFERENCES

1. Holcomb, Gary L. (1989), *A Direct Method for calculating Instrument Noise Levels in Side- by-Side Seismometer Evaluations*, DOI USGS Open-File Report 89-214.
2. Geotech Instruments, *GS-13BH Datasheet*, July 2009.
3. IEEE Standard for Digitizing Waveform Recorders, IEEE Std. 1057-1994.
4. IEEE Standard for Analog to Digital Converters, IEEE Std. 1241-2010.
5. Merchant, B. John, and Darren M. Hart (2011), *Component Evaluation Testing and Analysis Algorithms*, SAND2011-8265.
6. Sleeman, R., Wettum, A., Trampert, J. (2006), *Three-Channel Correlation Analysis: A New Technique to Measure Instrumental Noise of Digitizers and Seismic Sensors*, Bulletin of the Seismological Society of America, Vol. 96, No. 1, pp. 258-271, February 2006.Appendix A: Amplitude and Phase Response

APPENDIX A: RESPONSE MODELS

3.1 STS-2 Reference Sensor Response

Streckheisen STS-2 serial number 120651 is a third generation STS-2.

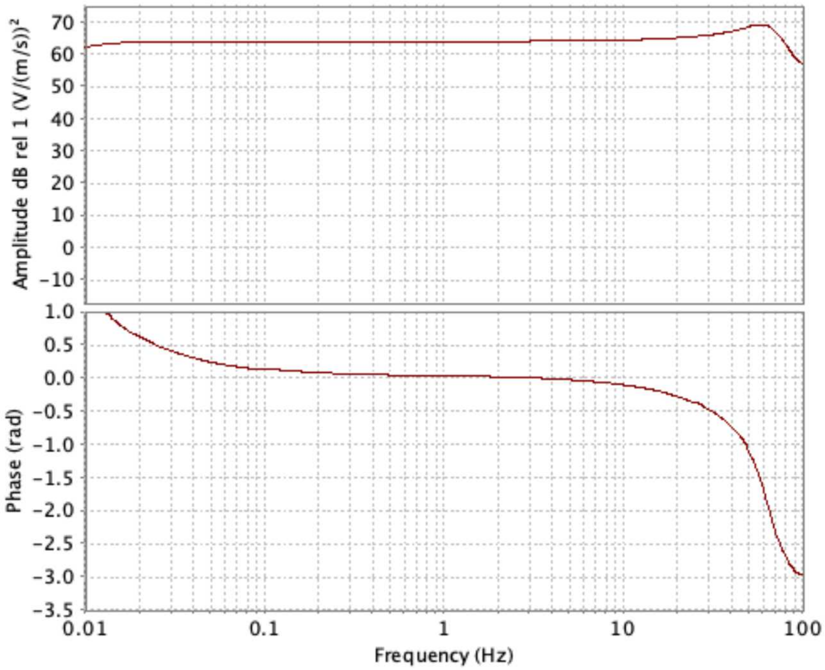

Sensitivity:
1,495.5 V·s/m at 1.0 Hz

Poles:

-13300.0	0.0
-10530.0	-10050.0
-10530.0	10050.0
-520.3	0.0
-374.8	0.0
-255.097	0.0
-97.34	-400.7
-97.34	400.7
-15.64	0.0
-0.037	-0.037
-0.037	0.037

Zeros:

-463.1	-430.5
-463.1	430.5
-176.6	0.0
-15.15	0.0
0.0	0.0
0.0	0.0

A:
518.69905E12 MV·s/m

DISTRIBUTION

Name	Org.	Sandia Email Address
Technical Library	9536	libref@sandia.gov

Sandia National Laboratories